JOURNAL OF COMPUTATIONAL PHYSICS 66, 239–249 (1986)

A Time-Implicit Monte Carlo Collision Algorithm for Particle-in-Cell Electron Transport Models*

C. W. CRANFILL, J. U. BRACKBILL, AND S. R. GOLDMAN

Los Alamos National Laboratory, Los Alamos, New Mexico 87545

Received September 6, 1985; revised December 10, 1985

A time-implicit Monte Carlo collision algorithm has been developed to allow particle-in-cell electron transport models to be applied to arbitrarily collisional systems. The algorithm is formulated for electrons moving in response to electric and magnetic accelerations and subject to collisional drag and scattering due to a background plasma. The correct fluid or streaming transport results are obtained in the respective limits of strongly or weakly collisional systems, and reasonable behavior is produced even for time-steps greatly exceeding the magnetic-gyration and collisional-scattering times. © 1986 Academic Press, Inc.

0. INTRODUCTION

In the study of transient phenomena in plasmas, a model for the transport of electrons is crucial. Such a model consists of a set of equations describing the electron motions combined with a set of algorithms for solving those equations. Typically, the equations of motion are some form of Newton's Laws with suitable driving forces, and the solution algorithms frequently must be performed numerically on a high-speed computer. For individual electrons, the driving forces consist of a slowly varying Lorentz force, due to ambient electric and magnetic fields, and a rapidly varying collisional force, due to screened-Coulomb interactions. For aggregates of electrons, additional driving forces can occur due to spatial gradients in the electron properties.

Plasmas experience transients with a wide range of characteristic time scales. The simplest algorithms for discretizing and solving the plasma equations of motion calculate the electron transport during a time-step using the initial values of the driving forces. These "time-explicit" algorithms are stable and accurate only for time-steps smaller than the shortest transient time scales allowed, so they are impractical for following the long-time evolution of most plasmas. Such time-step

581/66/1-16

0021-9991/86 $3.00

constraints are avoided by "time-implicit" algorithms, which calculate the electron transport during a time-step using time-advanced values of the driving forces.

Successful transport models incorporating time-implicit solution algorithms are well established for two limiting cases—the fluid limit, where electrons experience many collisions during a characteristic time, and the streaming limit, where electrons experience no collisions during a characteristic time. In the fluid limit, the electrons can be treated as an aggregate whose properties are described by the magnetohydrodynamic (MHD) equations, which produce transport fluxes driven by the Lorentz force and by density and temperature gradients and resisted by collisional drag and scattering. Time-implicit algorithms have been available for some time to numerically solve the resulting diffusive transport equations [1]. In the streaming limit, the electrons respond individually to the local Lorentz force, and the transport fluxes are accumulations of the individual electron orbits. Time-implicit particle-in-cell (PIC) algorithms have recently become available to solve Newton's Laws directly for the electron orbits using the implicit moment method to estimate time-advanced values for the fields producing the Lorentz force [2].

For more general cases that do not conform to either of these limits, satisfactory models have been more elusive. The best success has been achieved with hybrid models, which combine MHD algorithms to describe strongly collisional electrons with PIC algorithms to describe weakly collisional electrons [3]. Such hybrid models supplement their PIC algorithms with a Monte Carlo collision algorithm, which determines the effect of collisions on each electron orbit from a sequence of random numbers whose probability distribution is chosen to preserve the average properties of the collisional force. Up to now, only time-explicit Monte Carlo collision algorithms based on the seminal work of Shanny, Dawson, and Greene [4] have been available.

This report describes a time-implicit Monte Carlo collision algorithm for use with PIC electron transport schemes. The key innovation is to represent collisional scattering as a statistical rotation of the momentum vector, a technique similar to that used by Rechester and Rosenbluth [5] to treat stochastic magnetic fields. The statistical rotation is constrained to satisfy a generalized Ohm's Law on the average, so the correct diffusive transport is produced in the fluid limit even for time-steps greatly exceeding the magnetic-gyration and collisional-scattering times. The algorithm thus provides a smooth interpolation between the fluid and streaming limits.

The remainder of the report is organized in four sections and an appendix: Section 1 presents the basic electron equations of motion and a discretized solution algorithm; Section 2 describes the Monte Carlo collision algorithm; Section 3 derives the equivalent fluid equations resulting from ensemble averages of the electron equations of motion; Section 4 gives some examples of results; and the Appendix contains some algebra necessary to determine a statistical rotation vector satisfying the generalized Ohm's Law on the average.

1. Electron Equations of Motion

Consider an electron with mass m and charge $-e$ whose instantaneous position, momentum, and kinematic energy at time t are $\mathbf{r}(t)$, $\mathbf{p}(t)$, and $\varepsilon(t) \equiv \sqrt{(\mathbf{p}\cdot\mathbf{p}c^2 + m^2c^4)}$, where c is the speed of light. If the electron experiences local electric and magnetic fields $\mathbf{E}(\mathbf{r})$ and $\mathbf{B}(\mathbf{r})$ and collisional drag and deflection rates $\dot{I}(\mathbf{r}, \mathbf{p})$ and $\dot{\boldsymbol{\theta}}(\mathbf{r}, \mathbf{p})$, then its relativistic equations of motion can be written

$$d\mathbf{r}/dt = \mathbf{p}c^2/\varepsilon, \tag{1a}$$

$$d\mathbf{p}/dt = \dot{\mathbf{F}} - \dot{I}\mathbf{p} - (\dot{\boldsymbol{\Omega}} + \dot{\boldsymbol{\theta}}) \times \mathbf{p}, \tag{1b}$$

where $\dot{\mathbf{F}} \equiv -e\mathbf{E}$ and $\dot{\boldsymbol{\Omega}} \equiv -e\mathbf{B}c/\varepsilon$. Note that collisional deflection is treated like magnetic gyration to simplify the form of the momentum equation. Unlike magnetic gyration, however, collisional deflection is considered to be a capricious process whose properties are best described statistically and whose average effect is to resist the forward progress of the electron. Thus if $\dot{N}(\mathbf{r}, \mathbf{p})$ is the average scattering (i.e., right-angle-deflection) rate, then $\dot{\boldsymbol{\theta}}$ must be chosen to satisfy the constraint $\langle \dot{\boldsymbol{\theta}} \times \mathbf{p} \rangle = \dot{N}\langle \mathbf{p} \rangle$, where angle brackets denote averages over many deflections. The treatment of collisional deflection as a constrained statistical rotation is the key innovation of this work and leads directly to a generalized Ohm's Law:

$$d\langle \mathbf{p} \rangle/dt = \dot{\mathbf{F}} - (\dot{I} + \dot{N})\langle \mathbf{p} \rangle - \dot{\boldsymbol{\Omega}} \times \langle \mathbf{p} \rangle. \tag{1c}$$

In general, the motion of the electron is determined by numerically integrating Eqs. (1) using discrete time-steps, and a time-implicit algorithm is desired to avoid severe time-step constraints when $|\dot{\boldsymbol{\Omega}}|$ and $\dot{N}$ are large. Consider two successive times t_0 and t_1, and for any function $f(t)$ define $f_0 \equiv f(t_0)$, $f_1 \equiv f(t_1)$, $\Delta f \equiv f_1 - f_0$, and $f' \equiv f_0 + 0.5\,\Delta f$. Then suitable discretized versions of Eqs. (1) are

$$\Delta\mathbf{r} = (\mathbf{p}'c^2/\varepsilon')\,\Delta t, \tag{2a}$$

$$\Delta\mathbf{p} = \mathbf{F} - I\mathbf{p}' - (\boldsymbol{\Omega} + \boldsymbol{\theta}) \times \mathbf{p}', \tag{2b}$$

$$\langle \Delta\mathbf{p} \rangle = \mathbf{F} - (I + N)\langle \mathbf{p}' \rangle - \boldsymbol{\Omega} \times \langle \mathbf{p}' \rangle, \tag{2c}$$

where $\mathbf{F} \equiv \dot{\mathbf{F}}'\,\Delta t$, $I \equiv \dot{I}'\,\Delta t$, $\boldsymbol{\Omega} \equiv \dot{\boldsymbol{\Omega}}'\,\Delta t$, $\boldsymbol{\theta} \equiv \dot{\boldsymbol{\theta}}'\,\Delta t$, and $N \equiv \dot{N}'\,\Delta t$. Note that Eqs. (2) are time-implicit since their right-hand sides contain the time-advanced momentum $\mathbf{p}'$. Furthermore, Eqs. (2a) and (2b) correctly give the electron energy change, $\Delta\varepsilon \equiv \Delta\mathbf{p}\cdot\mathbf{p}'c^2/\varepsilon' = \Delta\mathbf{p}\cdot\Delta\mathbf{r}/\Delta t$, as the work done on the electron with no contribution from magnetic gyration or collisional deflection. This allows the electron motion, which is governed by the half-time momentum $\mathbf{p}'$, to become diffusive in the fluid limit without any spurious energy loss.

It is convenient to introduce the quantities

$$\mathbf{s} \equiv (\mathbf{p}_0 + 0.5\mathbf{F})/(1 + 0.5\Gamma), \qquad s^2 \equiv \mathbf{s} \cdot \mathbf{s},$$
$$\boldsymbol{\alpha} \equiv 0.5(\boldsymbol{\Omega} + \boldsymbol{\theta})/(1 + 0.5\Gamma), \qquad \alpha^2 \equiv \boldsymbol{\alpha} \cdot \boldsymbol{\alpha},$$
$$\boldsymbol{\beta} \equiv 0.5\boldsymbol{\Omega}/(1 + 0.5\Gamma + 0.5N), \qquad \beta^2 \equiv \boldsymbol{\beta} \cdot \boldsymbol{\beta},$$
$$S \equiv (1 + 0.5\Gamma)/(1 + 0.5\Gamma + 0.5N).$$

Equations (2b) and (2c) can then be manipulated to give

$$\mathbf{p}' = \mathbf{s} - \boldsymbol{\alpha} \times \mathbf{p}' = (\mathbf{s} - \boldsymbol{\alpha} \times \mathbf{s} + \boldsymbol{\alpha}\boldsymbol{\alpha} \cdot \mathbf{s})/(1 + \alpha^2), \tag{3a}$$

$$\langle \mathbf{p}' \rangle = S\mathbf{s} - \boldsymbol{\beta} \times \langle \mathbf{p}' \rangle = S(\mathbf{s} - \boldsymbol{\beta} \times \mathbf{s} + \boldsymbol{\beta}\boldsymbol{\beta} \cdot \mathbf{s})/(1 + \beta^2). \tag{3b}$$

Thus $\mathbf{p}'$ and $\langle \mathbf{p}' \rangle$ depend, respectively, on the source vectors $\mathbf{s}$ and $S\mathbf{s}$ and on the rotation vectors $\boldsymbol{\alpha}$ and $\boldsymbol{\beta}$. Since $\boldsymbol{\alpha}$ contains the collisional deflection vector $\boldsymbol{\theta}$, it is to be chosen statistically with its average properties constrained by Eq. (3b).

Equations (2a) and (3a) constitute a discretized solution algorithm for the electron equations of motion. A Monte Carlo collision algorithm for choosing the rotation vector $\boldsymbol{\alpha}$ subject to Eq. (3b) is described in Section 2. Reasonable results in both the fluid and streaming limits lend credibility to this solution algorithm. In the fluid limit ($N \gg 1$), the rotation vector $\boldsymbol{\beta}$ reduces to the Hall coefficient $\boldsymbol{\Omega}/N$, and Eq. (3b) gives currents parallel, perpendicular, and transverse to the magnetic field which depend on this parameter in just the way dictated by MHD theory. In the streaming limit ($\Gamma = N = 0$, $\boldsymbol{\theta} = 0$), the rotation vectors satisfy $\boldsymbol{\alpha} = \boldsymbol{\beta} = 0.5\boldsymbol{\Omega}$, and Eq. (3a) gives the detailed electron gyro-orbits when $|\boldsymbol{\Omega}| < 1$ and reduces to a zero-gyro-radius approximation when $|\boldsymbol{\Omega}| \gg 1$. Note that the zero-gyro-radius approximation fails to reproduce field-gradient drifts, but these drifts can be recovered by adding a diamagnetic term to the electric field in the source vector $\mathbf{s}$ without affecting the collision algorithm [2].

2. Monte Carlo Collision Algorithm

The collision terms in Eqs. (1) are appropriate for a fast electron moving through a stationary background plasma. In this case the predominant collisions are due to the screened-Coulomb interaction, a long-range force that produces finite effects as accumulations of many small random effects. Collisional drag directly affects the electron kinematic energy, so accurate results can be obtained from the discretized equations (2) only if the time-step is sufficiently small that $\Gamma < 1$. Collisional scattering, on the other hand, tends simply to isotropize the electron motion, so accurate results should be possible even when $N > 1$, where a large deflection of the electron path during the time-step must be interpreted as an accumulation of many small random deflections. Thus while collisional drag can be treated as a con-

tinuous process, collisional deflection is best described as a discrete random process, which is simulated numerically by the Monte Carlo procedure of selecting deflections from a random-number sequence whose probability distribution is chosen to preserve the average properties of the screened-Coulomb collisional force.

Collisional deflection enters the discretized solution algorithm for the electron equations of motion through the rotation vector $\boldsymbol{\alpha}$ appearing in Eq. (3a), so the collision algorithm must contain a Monte Carlo procedure for choosing $\boldsymbol{\alpha}$ subject to the constraint equation (3b). The algebra can be simplified by separating $\boldsymbol{\alpha}$ and $\boldsymbol{\beta}$ into components parallel and perpendicular to the source direction $\hat{s} \equiv \mathbf{s}/s$ as follows:

$$\alpha_s \equiv \boldsymbol{\alpha} \cdot \hat{s} = \boldsymbol{\alpha} \cdot \mathbf{p}'/s, \qquad \beta_s \equiv \boldsymbol{\beta} \cdot \hat{s} = \boldsymbol{\beta} \cdot \langle \mathbf{p}' \rangle / Ss,$$

$$\boldsymbol{\alpha}_\dagger \equiv (\boldsymbol{\alpha} - \alpha_s \hat{s} + \alpha_s \boldsymbol{\alpha} \times \hat{s})/(1 + \alpha_s^2), \qquad \alpha_\dagger^2 \equiv \boldsymbol{\alpha}_\dagger \cdot \boldsymbol{\alpha}_\dagger = (\alpha^2 - \alpha_s^2)/(1 + \alpha_s^2),$$

$$\boldsymbol{\beta}_\dagger \equiv (\boldsymbol{\beta} - \beta_s \hat{s} + \beta_s \boldsymbol{\beta} \times \hat{s})/(1 + \beta_s^2), \qquad \beta_\dagger^2 \equiv \boldsymbol{\beta}_\dagger \cdot \boldsymbol{\beta}_\dagger = (\beta^2 - \beta_s^2)/(1 + \beta_s^2).$$

The perpendicular components were chosen to satisfy $\boldsymbol{\alpha}_\dagger \cdot \mathbf{p}' = 0$ and $\boldsymbol{\beta}_\dagger \cdot \langle \mathbf{p}' \rangle = 0$, and this decomposition allows Eqs. (3) to be reduced to

$$\mathbf{p}' = \mathbf{s} - \boldsymbol{\alpha}_\dagger \times \mathbf{p}' = (\mathbf{s} - \boldsymbol{\alpha}_\dagger \times \mathbf{s})/(1 + \alpha_\dagger^2), \tag{4a}$$

$$\langle \mathbf{p}' \rangle = S\mathbf{s} - \boldsymbol{\beta}_\dagger \times \langle \mathbf{p}' \rangle = S(\mathbf{s} - \boldsymbol{\beta}_\dagger \times \mathbf{s})/(1 + \beta_\dagger^2). \tag{4b}$$

Thus the collision algorithm need only contain a Monte Carlo procedure for choosing $\boldsymbol{\alpha}_\dagger$ such that

$$\langle 1/(1 + \alpha_\dagger^2) \rangle = S/(1 + \beta_\dagger^2), \tag{5a}$$

$$\langle \boldsymbol{\alpha}_\dagger/(1 + \alpha_\dagger^2) \rangle = S\boldsymbol{\beta}_\dagger/(1 + \beta_\dagger^2). \tag{5b}$$

Some guidance is obtained from the case $\boldsymbol{\Omega} = 0$, for which collisional deflection of the electron path during the time-step is symmetric about $\hat{s}$ and can be represented by spherical rotation angles θ, ϕ. If $\hat{s}_\dagger$ is any unit vector perpendicular to $\hat{s}$, then

$$\boldsymbol{\alpha}_\dagger = \tan(0.5\theta)(-\sin\phi \hat{s}_\dagger + \cos\phi \hat{s} \times \hat{s}_\dagger),$$

where ϕ is uniformly probable on $[0, 2\pi]$ and θ has a probability distribution on $[0, \pi]$ such that $\langle \cos^2(0.5\theta) \rangle = S$. Since θ is the accumulation of many small random deflections, the central limit theorem of probability theory guarantees that its distribution will be some sort of Gaussian. While a Gaussian distribution can be imposed at each time-step, this seems unnecessary since the central limit theorem also guarantees that any member of a broad class of distributions for θ will produce a Gaussian distribution for the accumulation of θ over several time-steps. Thus the probability distribution for θ can be chosen somewhat arbitrarily.

For the case $\boldsymbol{\Omega} \neq 0$, magnetic gyration will contribute to the deflection of the elec-

tron path during the time-step, and the symmetry about $\hat{s}$ will be broken. The simplest way to generalize the $\boldsymbol{\Omega} = 0$ expression for $\boldsymbol{\alpha}_\dagger$ is to add the magnetic gyration vector (see Appendix):

$$\boldsymbol{\alpha}_\dagger = \boldsymbol{\beta}_\dagger / S + \tan(0.5\theta)(-\sin\phi \hat{s}_\dagger + \cos\phi \hat{s} \times \hat{s}_\dagger), \tag{6}$$

where ϕ is again uniformly probable on $[0, 2\pi]$ and θ must be chosen such that $\cos^2(0.5\theta) = S^2/(S + \beta_\dagger^2 - S\beta_\dagger^2)$ to satisfy the constraint equations (5). While a deterministic choice for θ may seem to place excessive faith in the arbitrariness of the θ distribution, expression (6) with only ϕ chosen randomly works surprisingly well for all cases having $\beta < 0.5$. When $\beta > 0.5$, however, collisions fail to partition the electron energy equally among the three spatial degrees of freedom even after many collision times—energy is depleted from the direction parallel to the magnetic field. Several more complicated expressions for $\boldsymbol{\alpha}_\dagger$ have been examined, but none has yet been found which allows collisions to equipartition the electron energy for large values of β, so the simple expression (6) has been used for all the examples of results given in Section 4. Note that the condition $\beta < 0.5$ is automatically satisfied unless $|\boldsymbol{\Omega}| > 0.5(\Gamma + N)$, in which case the time-step must be constrained to ensure that $|\boldsymbol{\Omega}| - 0.5(\Gamma + N) < 1$.

3. Equivalent Fluid Equations

The new time-implicit Monte Carlo collision algorithm is meant to allow PIC electron transport models to be applied to arbitrarily collisional systems, so it is useful to examine the fluid limit, in which the electron properties of interest are the local charge and current densities. Since these densities are defined as accumulations of many individual electron orbits, they can be treated as continuous functions and are governed by the equivalent fluid equations resulting from ensemble averages of the electron equations of motion. These ensemble averages reproduce the continuity equation and generalized Ohm's Law characteristic of MHD models.

This can be illustrated by considering an ensemble of nonrelativistic electrons in a small cell volume surrounding some position $\mathbf{r}$ at time t. Let the ith electron in the ensemble have position $\mathbf{r}_i(t)$ and velocity $\mathbf{v}_i(t)$ and contribute to the aggregate properties at position $\mathbf{r}$ through a weight function $w_i(\mathbf{r}, t)$, where w_i depends on position and time only through the quantity $\mathbf{r} - \mathbf{r}_i(t)$. The accumulated charge and current densities and the electron pressure and resistivity tensors are defined by

$$q(\mathbf{r}, t) \equiv -e \sum w_i(\mathbf{r}, t), \qquad \mathbf{j}(\mathbf{r}, t) \equiv -e \sum \mathbf{v}_i w_i(\mathbf{r}, t),$$

$$\mathbf{P}(\mathbf{r}, t) \equiv m \sum \mathbf{v}_i \mathbf{v}_i w_i(\mathbf{r}, t), \qquad \dot{\boldsymbol{\eta}} \cdot \mathbf{j}(\mathbf{r}, t) \equiv -e \sum (\dot{\Gamma}_i + \dot{N}_i)\, \mathbf{v}_i w_i(\mathbf{r}, t),$$

where $\sum$ represents a summation over all the electrons in the ensemble. The non-

relativistic versions of the electron equations of motion (1) along with the relation $\partial w_i/\partial t = -\mathbf{v}_i \cdot \nabla w_i$ then give

$$\partial q/\partial t = -\nabla \cdot \mathbf{j}, \tag{7a}$$

$$\partial \mathbf{j}/\partial t = (-e/m)(q\mathbf{E} + \mathbf{j} \times \mathbf{B}/c - \nabla \cdot \mathbf{P}) - \dot{\boldsymbol{\eta}} \cdot \mathbf{j}, \tag{7b}$$

where ∇ is the spatial gradient. Equations (7) constitute the equivalent fluid equations for the ensemble and are indeed seen to be the continuity equation and generalized Ohm's Law of MHD theory. In the notation of Section 1, time-implicit discretized versions of Eqs. (7) are

$$\Delta q = (-\nabla \cdot \mathbf{j}')\,\Delta t, \tag{8a}$$

$$\Delta \mathbf{j} = (-e/m)(q'\mathbf{E}' + \mathbf{j}' \times \mathbf{B}'/c - \nabla \cdot \mathbf{P}_0)\,\Delta t - \dot{\boldsymbol{\eta}}_0 \cdot \mathbf{j}'\,\Delta t. \tag{8b}$$

The pressure and resistivity tensors are evaluated at time t_0 to avoid having to estimate the time-advanced electron orbits. Time-advanced values of the charge and current densities can then be obtained by solving Eqs. (8) for $q' = q_0 + 0.5\,\Delta q$ and $\mathbf{j}' = \mathbf{j}_0 + 0.5\,\Delta \mathbf{j}$.

4. Examples of Results

To demonstrate the salient features of the time-implicit Monte Carlo collision algorithm, some examples of results are shown in Figs. 1–3. These examples represent the average response of 400 electrons to various constant electric, magnetic, and collisional accelerations. For a given set of accelerations, all electrons were initialized identically and moved according to Eqs. (2a), (4a), and (6), so the only differences in the electron motions were due to the random choices for the azimuthal collisional deflection angle ϕ. For all examples, the collisional drag rate was set to zero and the collisional scattering rate was set to one inverse time unit. The initial electron motion was along a coordinate axis, any nonzero electric field was along the same coordinate axis, and any nonzero magnetic field was along a different coordinate axis. The electron motions were followed for 1000 time units.

Figure 1 compares the time-dependent mean-squared electron displacements using time-steps of (a) one time unit and (b) ten time units when the electric and magnetic fields are zero. In either case, the total mean-squared displacement and its components along the three coordinate axes are straight lines as would be obtained from a random-walk diffusion, and the motion is isotropic since the three components overlie one another. Furthermore, the total mean-squared displacements after 1000 time units in the two cases differ by only 1% (2114 compared to 2088). Thus the time-implicit collision algorithm produces an accurate result using a ten-fold larger time-step than a time-explicit collision algorithm could safely use.

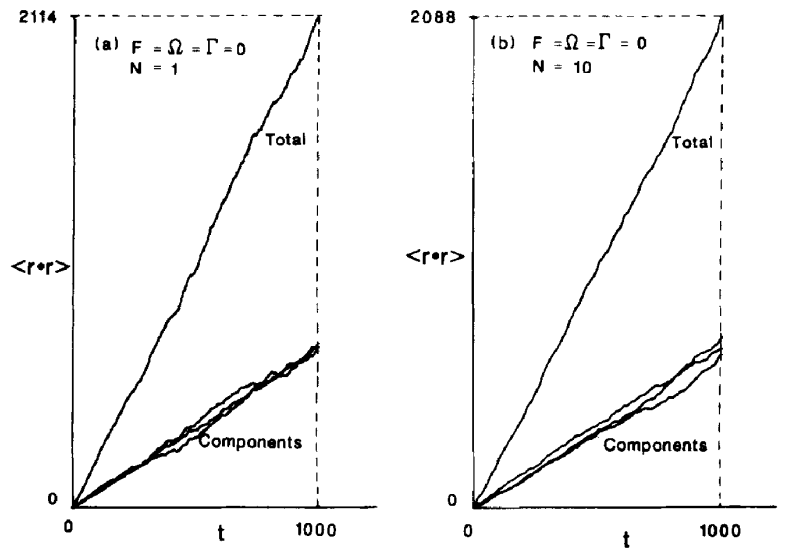

FIG. 1. Mean-squared displacements versus time for a random-walk diffusion. (a) Time-step is one scattering time. (b) Time-step is ten scattering times.

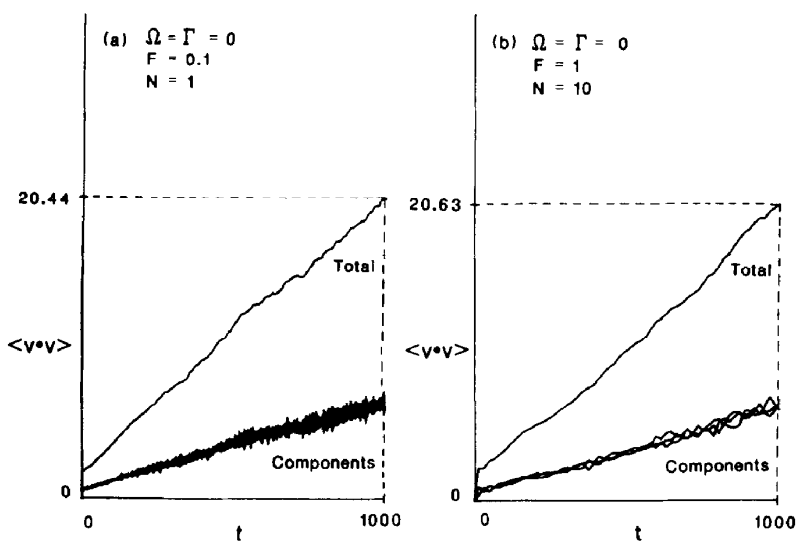

FIG. 2. Mean-squared velocities versus time for an Ohmic dissipation. (a) Time-step is one scattering time. (b) Time-step is ten scattering times.

Figure 2 compares the time-dependent mean-squared electron velocities using time-steps of (a) one time unit and (b) ten time units when the magnetic field is zero but the electric field is finite. In either case, the total mean-squared velocity and its components along the three coordinate axes are straight lines as would be obtained from an Ohmic dissipation, and the energy has been equipartitioned since the three components overlie one another. Furthermore, the total mean-squared velocities after 1000 time units in the two cases differ by only 1% (20.44 versus 20.63). Thus the time-implicit collision algorithm again produces an accurate result using a ten-fold larger time step than a time-explicit collision algorithm could safely use.

Figure 3 compares the time-dependent mean-squared electron velocities using magnetic fields such that (a) $\beta = 0.5$ and (b) $\beta = 1$ when the time-step is ten time units and the electric field is zero. In either case, the total mean-squared velocity is constant reflecting energy conservation during magnetic gyration and collisional deflection, but the energy is not equipartitioned since the components along the three coordinate axes do not overlie one another. The component along the magnetic field axis is depleted slightly for $\beta = 0.5$ and grossly for $\beta = 1$, and this illustrates the requirement $\beta < 0.5$ mentioned in Section 2. It is possible that this constraint can be removed by choosing the polar collisional deflection angle θ randomly rather than deterministically, but this has yet to be proven.

The above examples demonstrate that the time-implicit Monte Carlo collision algorithm produces reasonable behavior in the fluid limit even for time-steps greatly exceeding the magnetic-gyration and collisional-scattering times. Since the collision

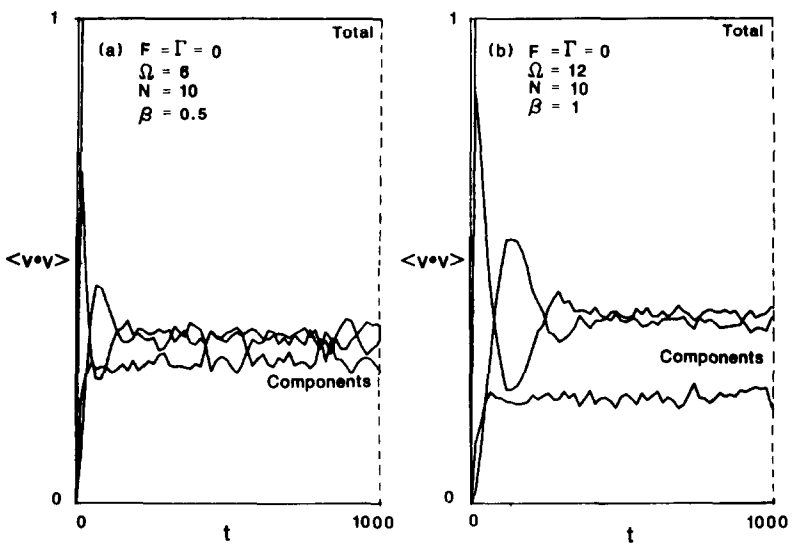

FIG. 3. Mean-squared velocities versus time for a magnetic gyration with collisional deflection. (a) $\beta = 0.5$. (b) $\beta = 1.0$.

algorithm also produces reasonable behavior in the streaming limit, it is hoped that it will allow PIC electron transport models to be applied to arbitrarily collisional systems.

APPENDIX: Statistical Rotation Vector

The statistical rotation vector must combine a deterministic magnetic gyration with a probabilistic collisional deflection subject to the constraint that a generalized Ohm's Law be satisfied on the average. Equations (4) show that only the components of the rotation vector perpendicular to the source direction need be determined, but the algebra is complicated by the nonlinear nature of the constraint equations (5). It is thus not obvious that Eq. (6), a linear superposition of a magnetic gyration and a collisional deflection, yields a suitable rotation vector.

To verify that it does, introduce the quantities σ and $\boldsymbol{\gamma}_\dagger \equiv \gamma_\dagger \hat{s}_\dagger$ and let

$$\boldsymbol{\alpha}_\dagger = \boldsymbol{\gamma}_\dagger/\sigma + \tan(0.5\theta)(-\sin\phi\hat{s}_\dagger + \cos\phi\hat{s}\times\hat{s}_\dagger), \tag{A1a}$$

$$1+\alpha_\dagger^2 = \sec^2(0.5\theta) + \gamma_\dagger^2/\sigma^2 - (2\gamma_\dagger/\sigma)\tan(0.5\theta)\sin\phi \equiv a - b\sin\phi, \tag{A1b}$$

where ϕ is to be uniformly probable on $[0, 2\pi]$. Averaging over ϕ gives

$$\langle 1/(1+\alpha_\dagger^2)\rangle_\phi = 1/\sqrt{(a^2-b^2)}, \tag{A2a}$$

$$\langle \boldsymbol{\alpha}_\dagger/(1+\alpha_\dagger^2)\rangle_\phi = [\gamma_\dagger/\sigma - (\sigma/2\gamma_\dagger)(a-\sqrt{(a^2-b^2)})]\,\hat{s}_\dagger/\sqrt{(a^2-b^2)}. \tag{A2b}$$

Choosing $\gamma_\dagger \equiv \gamma_\dagger/\sigma - (\sigma/2\gamma_\dagger)(a-\sqrt{(a^2-b^2)})$ then gives $1+\gamma_\dagger^2 = \sigma\sqrt{(a^2-b^2)}$ and $\tan^2(0.5\theta) = (1-\sigma)(\sigma+\gamma_\dagger^2)/\sigma^2$, so Eqs. (A2) reduce to

$$\langle 1/(1+\alpha_\dagger^2)\rangle_\phi = \sigma/(1+\gamma_\dagger^2), \tag{A3a}$$

$$\langle \boldsymbol{\alpha}_\dagger/(1+\alpha_\dagger^2)\rangle_\phi = \sigma\boldsymbol{\gamma}_\dagger/(1+\gamma_\dagger^2). \tag{A3b}$$

Equations (5) then show that further averaging over θ must give

$$\langle \sigma/(1+\gamma_\dagger^2)\rangle_\theta = S/(1+\beta_\dagger^2), \tag{A4a}$$

$$\langle \sigma\boldsymbol{\gamma}_\dagger/(1+\gamma_\dagger^2)\rangle_\theta = S\boldsymbol{\beta}_\dagger/(1+\beta_\dagger^2). \tag{A4b}$$

The simplest choice is $\sigma = S$ and $\boldsymbol{\gamma}_\dagger = \boldsymbol{\beta}_\dagger$, which gives $\cos^2(0.5\theta) = S^2/(S+\beta_\dagger^2 - S\beta_\dagger^2)$ and verifies Eq. (6).

REFERENCES

1. J. U. BRACKBILL AND S. R. GOLDMAN, *Commun. Pure Appl. Math.* **36** (1983), 415.
2. J. U. BRACKBILL AND D. W. FORSLUND, "Simulation of Low Frequency Electromagnetic Phenomena in Plasmas," *Multiple Time Scales*, edited by J. U. Brackbill and B. I. Cohen (Academic Press, New York, 1985), p. 271.
3. R. J. MASON, "Hybrid and Collisional Implicit Plasma Simulation Models," *Multiple Time Scales*, edited by J. U. Brackbill and B. I. Cohen (Academic Press, New York, 1985), p. 233; J. DENAVIT, "Time-Implicit Simulation of Particle-Fluid Systems," *Space Plasma Simulations*, edited by M. Ashour-Abdalla and D. A. Dutton (Reidel, Dordrecht, 1985).
4. R. SHANNY, J. M. DAWSON, AND J. M. GREENE, *Phys. Fluids* **10** (1967), 1281.
5. A. B. RECHESTER AND M. N. ROSENBLUTH, *Phys. Rev. Lett.* **40** (1978), 38.